# Iterative Equalization/Decoding of LDPC code transmitted over MIMO Fading ISI Channels

Heung-no Lee and Vivek Gulati
Information Science Laboratory in HRL Laboratories LLC, Malibu;
E-mail: hnlee@ee.pitt.edu

*Abstract*— **We propose a spectrum efficient and robust *space-time-frequency* code system for a $(N_t, N_r)$ MIMO, $L+1$-tap fading channel. The LDPC code is employed at the transmitter and iterative maximum *a posteriori* (MAP) equalizers are used at the receiver. We propose a novel, reduced-complexity iterative decoding and equalization scheme in which we combine the message-passing decoder, on the Bipartite graph for LDPC code, with an iterative MAP equalizers in a turbo-like manner. First, we consider a full-complexity vector MAP equalizer which runs the forward/backward algorithm on the trellis which has $M^{N_t \times L}$ states with $M^{N_t}$ transitions from each state when an $M-$ary constellation is used. Second, we replace the full MAP with the bank of $N_t$ per-antenna MAP (PAMAP) equalizers–each works on a $M^L$ state trellis–and evaluate the performance loss due to the use of the reduced complexity scheme. The simulation results show that the performance of the PAMAP-Bipartite equalization/decoding scheme is very close to the full complexity vector MAP-Bipartite. In addition, in fast fading case, the performance of the proposed *space-time-frequency* system with $N_t = 2$ and $N_r = 2$ and $L = 2$ is very close, within 0.5 dB, to the results of LDPC code on AWGN channels.**

## I. Introduction

Wireless signals experience time-varying frequency-selective fading due to the combined effect of multipath propagation, mobility of transceivers and changing environments. Realizing the maximum diversity benefit, which may be available in space, frequency or time domain, is critical in designing robust transceivers for these harsh conditions. Spatial diversity at the receiver, frequency and time diversity have all been widely studied [1]. Recently, transmit diversity has received widespread attention sparked by the capacity calculations [2], [3] which promise a linear increase in capacity with the number of transmit antennas in a rich scattering channel environment.

The transmit diversity can be used to achieve a gain either in capacity or in SNR. For example, the BLAST architecture [4] utilizes the transmit diversity to obtain increased capacity and the Space-Time Trellis Codes [5] use it for getting a diversity SNR gain. In this paper, our focus is in the direction of coding, but with a more general assumption of a time-varying frequency-selective fading channel and with the use of block code.

The channel is modelled with $N_t$-transmit and $N_r$-receive antennas and each of the sub-channels from one transmit antenna to a receive antenna is modelled with $L+1$ fading intersymbol-interference (ISI) taps. Assuming all taps are independent from each other, we note that an additional frequency-diversity factor of up to $L+1$ can be realized with the employment of a good equalizer. In addition, we consider the use of the low density parity check (LDPC) code [6] as the underlying *space-time-frequency* coding scheme. In particular, the data sequence transmitted at each antenna is simply a subsequence of length $N_B$, a serial-to-parallel multiplexing of the LDPC codeword of length $N$, i.e. $N = N_t \times N_B$. For example, for a LDPC codeword $(d_0 d_2 \ldots d_{N-1})$, the subsequence $(d_0 d_{N_t} d_{2N_t} \ldots d_{(N_B-1)N_t})$ is transmitted at the first antenna. Thus, a single codeword of rate, $1/N_t$, is transmitted over the $N_t$ transmit antennas; thus, the overall data rate is $\log_2(M)$ bits/sec/Hz.

Frequency-selective channels introduce inter-symbol interference(ISI) into the transmit signals, but this may also be viewed as additional diversity available in the frequency domain. In order to exploit this benefit, the use of a good equalizer is essential[1]. In [7], a reduced-complexity iterative[2] per-antenna MAP (PAMAP) equalizer was proposed for the MIMO ISI fading channels. It was shown that the iterative PAMAP closely achieves, within a few dB, the performance of the full-complexity, non-iterative vector-MAP with 2 or 3 iterations for uncoded transmissions. Both equalizers were shown to exploit diversities available in both the spatial and frequency domains. The order of diversity[3] achieved is $N_r \times (L+1)$ for *direct transmission*[4], while realizing the rate $N_t \times log_2(M)$. In addition, it was also shown in [7] that the PAMAP can be used to exploit the maximum space-frequency diversity order of $N_t \times N_r \times (L+1)$ at the rate $log_2(M)$ by transmitting randomly interleaved versions of an original sequence at each transmit antenna.

For LDPC code, the message-passing decoder on a Bipartite graph is well known [8]. In this paper, we evaluate the two equalizers, the full-complexity MAP and the PAMAP scheme when they are turbo-iteratively combined with the Bipartite decoder scheme. We will refer to the combination of the bipartite graph decoder and the full complexity vector MAP equalizer as "MAP-Bipartite" and the other as "PAMAP-Bipartite". The simulation results show that the PAMAP-Bipartite approaches within 0.5dB the performance of the MAP-Bipartite with 5 iterations between the equalizer-block and the decoder.

The main contributions of the paper are the following. We propose a new *space-time-frequency* transceiver scheme based on the LDPC code. The PAMAP-Bipartite is a joint equalizer and decoder system; it provides a low complexity solution with a negligible performance loss compared to the full complexity MAP-Bipartite. It is shown that the proposed transceiver overcomes the problems of ISI, and achieves a remarkable coding gain. In simulation, we are able to show that the proposed transceiver system approaches, within 0.5 dB, the bit error rate performance of the LDPC code on AWGN channels, at

[1] There are other modulation technologies such as CDMA or OFDM which does not require an explicit time-domain equalization considered in this paper. However, they are not within the scope of this research.

[2] iterations among $N_t$ MAP equalizers

[3] The order of diversity in this paper is defined as the power-law exponent $D$, where error rate curves asymptotically decays as $\frac{1}{SNR^D}$

[4] transmitting independent stream of information at each transmit antenna

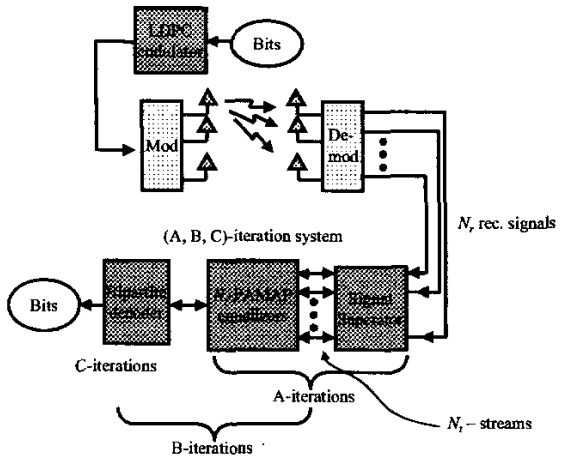


Fig. 1. The overview of the proposed space-time code/decoding system. This figure is explained more in Section V.

the normalized fading rate of 0.1. It should be noted that the channel at this fading rate provides an ample source of time-diversity benefit, and that the bipartite graph code is a strong time-diversity code by having edges of the graph randomly connecting the bit-nodes with the check-nodes. The proposed joint equalizer/decoder system is able to exploit this opportunity of achieving a large time-diversity benefit almost in full.

The rest of the paper is organized as follows. Section II discusses some previous studies on related topics. Section III describes the system model. The following section describes the proposed solution. Simulation results are presented in section V. We conclude with some remarks in section VI.

## II. Previous Work

Recently, there has been a lot of emphasis on joint equalization and decoding of coded systems. The application of the "turbo" principle[9], [10] to iterative decoding and demodulation has provided significant gains([11], [12], [13], [14], [15], [16], [17], [18]). Such systems are essentially serial concatenation schemes([19]) with the ISI channel as the inner code. By making the channel appear recursive([13]), significant interleaving gains are achievable. The decoding is done iteratively([20]) using variants of the MAP algorithm([21], [22]). The insights provided by density evolution and Gaussian approximation([23], [24], [25]) have led to better precoders for ISI channels[26].

In the context of multiple-input, multiple-output(MIMO) channels, Tarokh *et. al.* showed that space-time codes([27]) provide the maximum diversity order on flat-fading channels [28]. Heikkila *et al* [29] presented simulation studies on the performance of space-time trellis codes in fading ISI channels. Bauch and Naguib [30] presented the performance results of a space-time code over a 2-tap ISI channel. Their iterative scheme employed the BCJR algorithm for joint equalization and decoding.

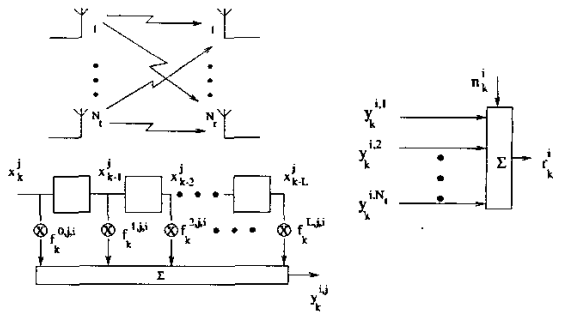

Fig. 2. The MIMO-ISI channel model.

## III. System Model

We consider the transmission of data through a time-varying, frequency-selective fading channel using $N_t$ transmit antennas, in blocks of size $N$. These $N \times N_t$ symbols are coded symbols in this paper. The channel is modelled as a symbol-spaced $L+1$ tap Rayleigh fading channel. Let $N_r$ be the number of receive antennas(Figure 2). The received signal on antenna $i$ at time instant $k$ is given by the super-position of the signals transmitted on each transmit antenna and the inter-symbol interference experienced by these symbols:

$$\begin{aligned} r_k^i &= \sum_{j=0}^{N_t}\left[\sum_{l=0}^{L} f_k^{l,j,i} x_{k-l}^j\right] + n_k^i \\ &= \sum_{j}^{N_t} y_k^{i,j} + n_k^i \\ &= y_k^i + n_k^i \end{aligned} \tag{1}$$

Thus, there are $M^{(L+1)N_t}$ possible values of $y_k^i$. It would be convenient to collect all the transmit and receive signals into column vectors:

$$\mathbf{x}_k = \begin{bmatrix} x_k^1 \\ x_k^2 \\ \vdots \\ x_k^{N_t} \end{bmatrix} \quad \text{and} \quad \mathbf{r}_k = \begin{bmatrix} r_k^1 \\ r_k^2 \\ \vdots \\ r_k^{N_r} \end{bmatrix}$$

Also, define the $N_r \times N_t$ matrix of "clean" signals as below:

$$\begin{aligned} \mathbf{Y}_k &= \begin{bmatrix} y_k^{1,1} & y_k^{1,2} & \cdots & y_l^{1,N_t} \\ y_k^{2,1} & y_k^{2,2} & \cdots & y_l^{2,N_t} \\ \vdots & \vdots & \ddots & \vdots \\ y_k^{N_r,1} & y_k^{N_r,2} & \cdots & y_l^{N_r,N_t} \end{bmatrix} \\ &= \begin{bmatrix} \mathbf{y}_k^1 \\ \mathbf{y}_k^2 \\ \vdots \\ \mathbf{y}_k^{N_r} \end{bmatrix} = \begin{bmatrix} \tilde{\mathbf{y}}_k^1 & \tilde{\mathbf{y}}_k^2 & \cdots & \tilde{\mathbf{y}}_k^{N_t} \end{bmatrix} \end{aligned}$$

Further, (1) may be re-written as:

$$\begin{aligned}
\mathbf{r}_k &:= \begin{bmatrix} r_k^1 \\ r_k^2 \\ \vdots \\ r_k^{N_r} \end{bmatrix} = \begin{bmatrix} y_k^1 + n_k^1 \\ y_k^2 + n_k^2 \\ \vdots \\ y_k^{N_r} + y_k^{N_r} \end{bmatrix} \\
&= \begin{bmatrix} y_k^{1,1} + y_k^{1,2} + \cdots + y_k^{1,N_t} \\ y_k^{2,1} + y_k^{2,2} + \cdots + y_k^{2,N_t} \\ \vdots \\ y_k^{N_r,1} + y_k^{N_r,2} + \cdots + y_k^{N_r,N_t} \end{bmatrix} + \begin{bmatrix} n_k^1 \\ n_k^2 \\ \vdots \\ n_k^{N_r} \end{bmatrix} \\
&= \begin{bmatrix} y_k^{1,1} \\ y_k^{2,1} \\ \vdots \\ y_k^{N_r,1} \end{bmatrix} + \begin{bmatrix} y_k^{1,2} \\ y_k^{2,2} \\ \vdots \\ y_k^{N_r,2} \end{bmatrix} + \cdots + \begin{bmatrix} y_k^{1,N_t} \\ y_k^{2,N_t} \\ \vdots \\ y_k^{N_r,N_t} \end{bmatrix} + \mathbf{n}_k \\
&= \tilde{\mathbf{y}}_k^1 + \tilde{\mathbf{y}}_k^2 + \cdots + \tilde{\mathbf{y}}_k^{N_t} + \mathbf{n}_k \qquad (2)
\end{aligned}$$

The fade coefficient $f_k^{l,j,i}$, representing the $l-$th tap between transmit antenna $j$ and receive antenna $i$ at time instant $k$, is a sample of a Rayleigh fading process. All the taps on all antennas are assumed to be fading independent of one another. The auto-correlation of all fading processes is assumed to be identical and depends only on the normalized Doppler rate. The power-delay profile is normalized:

$$\sum_{l=0}^{L} \mathrm{E}\left[\left|f_k^{l,j,i}\right|^2\right] = 1 \quad \forall i,j \qquad (3)$$
$$i = 1, \ldots, N_r \text{ and } j = 1, \ldots, N_t$$

where $E[x]$ denotes the expectation of $x$.

The transmit symbols $x_k^j$ belong to an $M-$ary constellation. Let $E_s$ be the energy of each transmit symbol. The noise samples $n_k^i$ are zero mean, complex Gaussian random variables with variance $N_0/2$ in each dimension. Signal-to-noise ratio(SNR) is defined in terms of the average SNR per bit. In the sequel we also assume that all the fades are known(perfect CSI). In practice, the fast fading channel taps may be estimated by employing, for example, snap-shot channel estimation using pilot symbols and interpolation [31].

## IV. Iterative MAP-Bipartite Equalizer/Decoder

In this section we first describe the full complexity, vector MAP-equalizer, which is a straightforward extension of the well known sequence-based MAP symbol estimation criterion [32], [21] to the MIMO ISI channel. Next, we describe the proposed low complexity, iterative per-antenna MAP (PAMAP) equalizer. Lastly, we describe the connection of the MAP equalizers to the message passing decoder on the Bipartite graph.

### A. Full Complexity Vector MAP Equalizer

The MAP equalizer makes a sequence-based decision on the transmit symbols using the maximum *aposteriori* criterion [32]. For our MIMO setting, this can be written as

$$\hat{\mathbf{x}}_k = \arg \max_{\mathbf{x} \in \Omega^{N_t}} \Pr\{\mathbf{x}_k | \mathbf{r}_j, j = 1, 2, \ldots, N\} \qquad (4)$$

where $\Omega$ denotes the $M-$ary signal constellation set. The probabilities involved in the maximization above are the soft information generated by the equalizer. Since the ISI channel is equivalent to a Markov process, the MAP rule may be described in terms of operations on a trellis. Each trellis transition, originating from a state $S_{s-1}$ and terminating in a state $S_s$, is marked with an input(or transmit) vector $\mathbf{x}^s$ and an output(or "clean") vector $\mathbf{y}^s$. The state at any time $k$ is defined completely by the $N_t \times L$ past signals. Let $\chi_x := \{(x_{k-1}, x_{k-2}, \ldots, x_{k-L}) : x_j \in \Omega\}$. Thus, the possible states belong to the set $\chi_x^{N_t}$, which has a cardinality $M^{LN_t}$. The output vectors may similarly be identified using the elements of the set $\chi_y^{N_t}$ where $\chi_y := \{(x_k, x_{k-1}, x_{k-2}, \ldots, x_{k-L}) : x_j \in \Omega\}$. The probability term in (4) is, thus, the sum of probabilities of making all the transitions that have $\mathbf{x}$ as the input vector at time epoch $k$:

$$\begin{aligned}
&\Pr\{\mathbf{x}_k | \mathbf{r}_j, j = 1, 2, \ldots, N\} \\
&= \sum_{\mathbf{m} \in \chi_x^{N_t}} \Pr(\mathbf{x}^s = \mathbf{x}_k, S_k = \mathbf{m} | \mathbf{r}_j, j = 1, 2, \ldots, N) \\
&= \frac{1}{\Pr(\mathbf{r}_j, j = 1, 2, \ldots, N)} \times \sum_{\mathbf{m}' \in \chi_x^{N_t}} \sum_{\mathbf{m} \in \chi_x^{N_t}} \\
&\quad \Pr\{\mathbf{x}^s = \mathbf{x}_k, S_{k-1} = \mathbf{m}', S_k = \mathbf{m}, \mathbf{r}_j, j = 1, 2, \ldots, N\} \\
&= K \sum_{\mathbf{m}'} \sum_{\mathbf{m}} \Pr(\mathbf{r}_j, j = k+1, \ldots, N | S_k = \mathbf{m}) \\
&\quad \times \Pr(S_{k-1} = \mathbf{m}' | \mathbf{r}_j, j = 1, \ldots, k) \\
&\quad \times \Pr(\mathbf{x}^s = \mathbf{x}_k, S_k = \mathbf{m}, \mathbf{r}_k | S_{k-1} = \mathbf{m}') \qquad (5)
\end{aligned}$$

The factor $K$ is just a constant normalization factor and the last decomposition follows from the Bayes rule and the Markovian property. Next, as in [20] we define the following probability functions:

$$\alpha_k(\mathbf{m}) = \Pr(S_k = \mathbf{m} | \mathbf{r}_j, j = 1, 2, \ldots, k) \qquad (6)$$
$$\beta_k(\mathbf{m}) = \frac{\Pr(\mathbf{r}_j, j = k+1, \ldots, N | S_k = \mathbf{m})}{\Pr(\mathbf{r}_j, j = k+1, \ldots, N | \mathbf{r}_j, j = 1, \ldots, k)} \qquad (7)$$
$$\gamma(\mathbf{x}^s, \mathbf{r}_k, \mathbf{m}', \mathbf{m}) = \Pr(\mathbf{x}_k = \mathbf{x}^s, S_k = \mathbf{m}, \mathbf{r}_k | S_{k-1} = \mathbf{m}') \qquad (8)$$

Thus, (5) may be rewritten as:

$$\begin{aligned}
&\Pr\{\mathbf{x}_k | \mathbf{r}_j, j = 1, 2, \ldots, N\} = \\
&\quad K \sum_{\mathbf{m}'} \sum_{\mathbf{m}} \alpha_{k-1}(\mathbf{m}') \gamma(\mathbf{x}^s, \mathbf{r}_k, \mathbf{m}', \mathbf{m}) \beta_k(\mathbf{m}) \qquad (9)
\end{aligned}$$

The quantities $\alpha_k(\mathbf{m})$ and $\beta_k(\mathbf{m})$ satisfy the following recursions [20], [21]

$$\alpha_k(\mathbf{m}) = \frac{\sum_{\mathbf{m}'} \sum_{\mathbf{x}^s} \gamma(\mathbf{x}^s, \mathbf{r}_k, \mathbf{m}', \mathbf{m}) \alpha_{k-1}(\mathbf{m}')}{\sum_{\mathbf{m}} \sum_{\mathbf{m}'} \sum_{\mathbf{x}^s} \gamma(\mathbf{x}^s, \mathbf{r}_k, \mathbf{m}', \mathbf{m}) \alpha_{k-1}(\mathbf{m}')} \qquad (10)$$
$$\beta_k(\mathbf{m}) = \frac{\sum_{\mathbf{m}'} \sum_{\mathbf{x}^s} \gamma(\mathbf{x}^s, \mathbf{r}_k, \mathbf{m}, \mathbf{m}') \beta_{k+1}(\mathbf{m}')}{\sum_{\mathbf{m}} \sum_{\mathbf{m}'} \sum_{\mathbf{x}^s} \gamma(\mathbf{x}^s, \mathbf{r}_k, \mathbf{m}, \mathbf{m}') \beta_{k+1}(\mathbf{m}')} \qquad (11)$$

The probability $\gamma(\mathbf{x}^s, \mathbf{r}_k, \mathbf{m}', \mathbf{m})$ may be written as a product of three terms:

$$\begin{aligned}
\gamma(\mathbf{x}^s, \mathbf{r}_k, \mathbf{m}', \mathbf{m}) &= p(\mathbf{r}_k | \mathbf{x}_k = \mathbf{x}^s, S_k = \mathbf{m}, S_{k-1} = \mathbf{m}') \\
&\quad \times q(\mathbf{x}_k = \mathbf{x}^s | S_k = \mathbf{m}, S_{k-1} = \mathbf{m}') \\
&\quad \times \pi(S_k = \mathbf{m} | S_{k-1} = \mathbf{m}') \qquad (12)
\end{aligned}$$

where $p(\cdot|\cdot)$ is the transition probability of the MIMO channel, $q(\mathbf{x}_k = \mathbf{x}^s | S_k = \mathbf{m}, S_{k-1} = \mathbf{m}')$ is a zero or a one depending on whether the transition from state $\mathbf{m}'$ to state $\mathbf{m}$ is marked with $\mathbf{x}_k$ or not and $\pi(S_k = \mathbf{m}|S_{k-1} = \mathbf{m}')$ is the *apriori* probability of this transition. The *apriori* probability is useful in a coded system where this information is obtained from the channel decoder. For LDPC code, we will describe the relationship in section IV-C.

There are a total of $M^{N_t \times L}$ states with $M^{N_t}$ transitions from each state. Thus, the complexity of this algorithm is of the order of $(M^{(L+1)N_t})$. This excludes the complexity involved in computing the transition probabilities $p(\mathbf{r}_k|\mathbf{x}_k = \mathbf{x}^s, S_k = \mathbf{m}, S_{k-1} = \mathbf{m}')$ from the received vectors $\mathbf{r}_k$.

### *B. Per-Antenna MAP Equalizer*

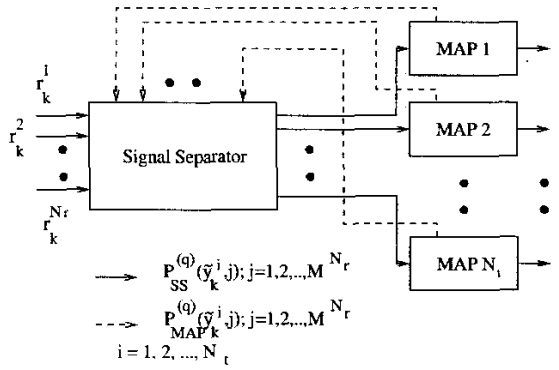


Fig. 3. The "per-antenna" MAP Equalizer.

The high complexity of the full MAP equalizer results from the fact that it searches the full state space $\mathbf{y}^i = y^{i,1} + y^{i,2} + \cdots + y^{i,N_t}, i = 1, 2, \ldots, N_r$. Each of the $y^{i,j}$ is the output of the channel which has $L$ memory elements. In this section, we develop a novel receiver structure that probabilistically singles out the contribution of a single transmit antenna, say $y^{i,j}, i = 1, 2, \ldots, N_r$, from the received signal $\mathbf{r}_k$ and then performs an MAP search on the reduced state space of $\tilde{\mathbf{y}}^j = [y^{1,j}\ y^{2,j}\ \ldots\ y^{N_r,j}]^T$.

The proposed equalizer consists of two parts – the signal separator and the per-antenna MAP bank. The signal separator generates the probabilities of the "clean signal" vectors $\tilde{\mathbf{y}}_k^i, i = 1, 2, \ldots, N_t$ from the received signal $\mathbf{r}_k$ as follows:

$$\Pr(\tilde{\mathbf{y}}_k^1 = \tilde{\mathbf{y}}_1, \tilde{\mathbf{y}}_k^2 = \tilde{\mathbf{y}}_2, \ldots, \tilde{\mathbf{y}}_k^{N_t} = \tilde{\mathbf{y}}_{N_t}|\mathbf{r}_k) = \frac{\Pr(\mathbf{r}_k|\tilde{\mathbf{y}}_k^1 = \tilde{\mathbf{y}}_1, \tilde{\mathbf{y}}_k^2 = \tilde{\mathbf{y}}_2, \ldots, \tilde{\mathbf{y}}_k^{N_t} = \tilde{\mathbf{y}}_{N_t})}{\Pr(\mathbf{r}_k)} \times \prod_{i=1}^{N_t} \Pr(\tilde{\mathbf{y}}_k^i = \tilde{\mathbf{y}}_i) \quad (13)$$

The term in the numerator is the transition probability of a MIMO channel. The term in the denominator is a constant and may be treated as a normalizing factor. Each of the terms in the product denotes the *apriori* probabilities. During the first iteration, all the symbols are assumed to be equally likely. During the later iterations, the extrinsic information obtained from the PAMAPs is treated as *apriori* information by the signal separator. Specifically, during the $q-$th iteration:

$$\Pr(\tilde{\mathbf{y}}_k^i = \tilde{\mathbf{y}}_i) = P_{\text{MAP}}^{(q-1)}(\tilde{\mathbf{y}}_k^i, i) \quad (14)$$

During the $q-$th iteration, the signal separator passes extrinsic information about the $\tilde{\mathbf{y}}_k^i$ to the PAMAPs:

$$P_{\text{SS}}^{(q)}(\tilde{\mathbf{y}}_k^i, i) = \Pr_{\text{ext}}(\tilde{\mathbf{y}}_k^i = \tilde{\mathbf{y}}_i) = \frac{1}{P_{\text{MAP}}^{(q-1)}(\tilde{\mathbf{y}}_k^i, i)} \times \sum_{\tilde{\mathbf{y}}_1} \cdots \sum_{\tilde{\mathbf{y}}_{i-1}} \sum_{\tilde{\mathbf{y}}_{i+1}} \cdots \sum_{\tilde{\mathbf{y}}_{N_t}} \{ \Pr(\tilde{\mathbf{y}}_k^1 = \tilde{\mathbf{y}}_1, \tilde{\mathbf{y}}_k^2 = \tilde{\mathbf{y}}_2, \ldots, \tilde{\mathbf{y}}_k^{N_t} = \tilde{\mathbf{y}}_{N_t}|\mathbf{r}_k) \} \quad (15)$$

where each $\tilde{\mathbf{y}}_i \in \chi_y^{N_r}$.

The per-antenna MAPs(PAMAPs) treat the extrinsic information generated by the signal separator as outputs of a channel(marked with solid lines in Fig. 3). The processing is identical to what has been described in the previous section. Each of these MAP filters now work on a trellis of only $M^L$ states and there are only $M$ transitions from each state. The trellises are now marked with symbols transmitted from a particular antenna, $x^s$, and the received vector $\tilde{\mathbf{y}}^s$. Thus, during the $q-$th iteration, the $j$-th PAMAP computes the probabilities:

$$\Pr\left\{ x_k^j = x^j \in \Omega \,\middle|\, P_{\text{SS}}^{(q)}(\tilde{\mathbf{y}}_t^j, i), t = 1, \ldots, N; i = 1, \ldots, M^{LN_r} \right\}$$

Once again, the kernel term for the $j-$th PAMAP may be computed easily:

$$\begin{aligned} &\gamma^j\{x^s, \tilde{\mathbf{r}}_k^j, \mathbf{m}', \mathbf{m}\} \\ &= \Pr(x_k^j = x^s, S_k = \mathbf{m}, \tilde{\mathbf{r}}_k^j | S_{s-1} = \mathbf{m}') \\ &= p(\tilde{\mathbf{r}}_k^j | x_k^j = x^s, S_k = \mathbf{m}, S_{k-1} = \mathbf{m}') \\ &\quad \times q(x_k^j = x^s | S_k = \mathbf{m}, S_{k-1} = \mathbf{m}') \\ &\quad \times \pi(S_k = \mathbf{m}|S_{k-1} = \mathbf{m}') \end{aligned} \quad (16)$$

where, with a slight abuse of notation, we may write:

$$p(\tilde{\mathbf{r}}_k^j | x_k^j = x^s, S_k = \mathbf{m}, S_{k-1} = \mathbf{m}') = P_{\text{SS}}^{(q)}(\tilde{\mathbf{y}}_k^j, j)$$

Further, the terms $\mathbf{m}$ and $\mathbf{m}'$ now take on values in the set $\chi_x$. The forward and the backward recursions for the PAMAPs are also straight-forward to write. In addition to the *aposteriori* probabilities of the transmit signals, these filters also compute the probability updates for the clean signals:

$$P_{MAP}^{(q)}(\tilde{\mathbf{y}}_k^i, i) = \Pr_{\text{ext}}(\tilde{\mathbf{y}}_k^i = \tilde{\mathbf{y}}_i) = \sum_{\mathbf{m},\mathbf{m}':\tilde{\mathbf{y}}_k^i = \tilde{\mathbf{y}}_i} \sum \frac{\alpha_{k-1}(\mathbf{m}')\gamma(\mathbf{x}^s, \tilde{\mathbf{r}}_k^i, \mathbf{m}', \mathbf{m})\beta_k(\mathbf{m})}{P_{\text{SS}}^{(q)}(\tilde{\mathbf{y}}_k^i, i)} \quad (17)$$

The extrinsic information thus generated by the PAMAPs is passed back to the signal separator(dashed lines in Fig. 3), which treats this information as *apriori* for the next iteration.

### C. Information Exchanged Between the Equalizer and the Bipartite Graph Decoder

In this section, we briefly describe the information passing system between the equalizer and the Bipartite Graph Decoder. We will only describe the more complex MAP-Bipartite system and then wish that the readers can straightforwardly follow up for the Bipartite-PAMAP system on their own, due to the limited space provided here.

Fig. 4 depicts a conceptual picture of the iterative decoding process of the Bipartite-MAP decoder/equalizer. First, we may start with the direction from the equalizer to the decoder. For each trellis-section, we have $N_t$ transmit symbols associated with it. Thus, we need to generate the $N_t$ extrinsic information from the output of the vector MAP equalizer. Specifically, we can easily obtain $\Pr\{\mathbf{x}_k = \mathbf{x} \in \Omega^{N_t} | \mathbf{r}_n, n = 1, 2, \ldots, N\}$ by considering (5). Then, we can single out the extrinsic information on the symbol at a particular antenna–say $j$-th–$x_k^j \in \Omega$, which can be computed as

$$P_{ext}(x_k^j = z) = \sum_{\mathbf{x} \in \Omega_t^N : x^j = z} \frac{\Pr(\mathbf{x}_k^j = \mathbf{x} | \mathbf{r}_n, n = 1, 2, \ldots, N)}{\prod_{q \neq j} P_{pr}(x_k^q = x^q)} \tag{18}$$

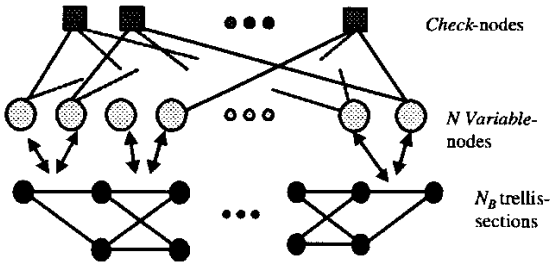


Fig. 4. Illustration of MAP-Bipartite iteration

We now continue for the direction from the decoder to the equalizer. Again referring to Fig. 4, we now need to combine the $N_t$ outputs of *variable* nodes from the Bipartite-graph decoder to generate the *a priori* probability $\pi(S_k = m | S_{k-1} = m')$, which can be easily computed by noting the following fact: Each of the event $\{S_k = m | S_{k-1} = m'\}$ has an associated input symbol vector as $\{x_k^1 = x^1, x_k^2 = x^2, \ldots, x_k^{N_t} = x^{N_t}\}$. Thus, we can generate $\pi\{S_k = m | S_{k-1} = m'\}$ by multiplying the $N_t$ a priori probabilities from the $N_t$ variable nodes associated with each of the trellis-sections.

Finally, the Bipartite-graph decoder uses the conventional iterative decoding scheme. For example, please refer to [23], [8] and reference therein.

## V. Simulation Results

We consider a system with $N_t = 2$ transmit antennas and $N_r = 1$ or 2 receive antennas. The channel is modeled with a three (i.e. $L = 2$) Rayleigh fading taps with a power delay profile $[\frac{1}{2}, \frac{1}{\sqrt{2}}, \frac{1}{2}]$. The modulation considered in this paper is BPSK. The frames consist of $N_B = 1024$ transmissions out of each antenna. The block code used is a rate 1/2 (3,6) regular LDPC code ([6]) with the block length $N = N_t \times N_B = 2048$. It should be noted that the overall rate of the system is thus $log_2(M = 2) = 1$ bit/sec/Hz. All the message passing metrics are implemented in the log-domain.

Referring to Fig. 1, we have an $(A, B, C)$-iteration system. For the simulation results given in this paper, we fixed $C = 10$, the number of iterations used for the Bipartite-graph decoder. In addition, relevant only to the PAMAP-Bipartite, $A$ is fixed to be 3–the number of iterations between the Signal Separator and the bank of $N_t$-PAMAP equalizer. Then, fig. 5 and 6 show the convergence speed of the proposed equalizers as $B$–the number of iterations between the equalizer and the decoder–is increased, for full MAP and for PAMAP respectively. The normalized fading rate, $f_{dm}T$ was 0.01 for these simulations. We note that both receiver converges very quickly as diminishing returns are noticeable after the 3rd-iteration. The performance degradation of PAMAP-Bipartite is very trivial, only about 0.5 dB away from the full MAP-Bipartite system.

It would be interesting to note the inherent time-diversity structure of the LDPC code. From examining the Parity-Tree (see Figure 2.5, pg 20, in Gallager's thesis [6]) spawned out of a symbol in a LDPC codeword, we note that a symbol in a codeword, is built to be dependent upon many symbols in other time-epochs. Therefore, the simulation results at different fading rates, $f_{dm}T = 0.001$ for Fig. 7 and $f_{dm}T = 0.1$ for 8, would serve as illustrative example to the concept of the built-in time-diversity structure of the LDPC code.

At the very slow fading rate of 0.001, the process of a channel tap essentially becomes quasi-static, thus the proposed system would not be able to exploit the time-diversity of the code, achieving only the space (the factor of $N_t \times N_r$) and frequency (the factor of $L + 1$) diversity and then the generic coding benefit on top of the diversity channel with an order of $D = N_t \times N_r \times (L + 1) = 12$. The curves labeled, $D = 6$ and $D = 12$, refer to the uncoded BER curves of BPSK matched filter bounds. We showed in [7] that for two receive-antenna system ($N_r = 2$), the uncoded PAMAP achieves the order of diversity $D = N_t * N_r * (L+1) = 12$ at 1 bit/sec/Hz with random-interleaved transmission of the same sequence at each antenna. This transmission scheme was a kind of repetitive channel coding. When more explicit channel code with the LDPC code is used, the overall system shall provide the coding benefit on top of the space-frequency diversity benefit of $D = 12$ at 1 bit/sec/Hz.

The fast-fading case simulation is shown in Fig. 8. At this fading rate, the channel tap gain is almost independent from one time epoch to other. Thus, the LDPC code is now be able to exploit almost all the time-diversity benefit available in the channel. The time diversity order of the system becomes very large since it is proportional to the length of the LDPC code. We know that when the order of diversity is large $D = \infty$, the underlying channel essentially becomes a AWGN channel. Applying the LDPC code to this almost AWGN, we will expect to obtain a performance result which would be very much similar to the system with the LDPC code on AWGN channel. Consequently, for $N_r = 2$ system we have the performance of the overall system very close, within 0.5 dB, to that of the LDPC applied to

AWGN channel.

The rest of the figures, Fig. 9 and 10, shows the frame error rates.

## VI. Conclusions

We have proposed a low-complexity iterative PAMAP-Bipartite equalizer/decoder scheme for the system in which the LDPC code is used as a space-time-frequency code in MIMO fading ISI channels. We have shown that the proposed transceiver system achieves all the diversity available in the channel, in space, time and frequency domains. The proposed system with $N_t = 2$ transmit and $N_r = 2$ receive antennas, and with $L+1 = 3$ tap channels, at the fast fading case achieves the bit error rate that are within 0.5 dB performance of the LDPC code on AWGN.

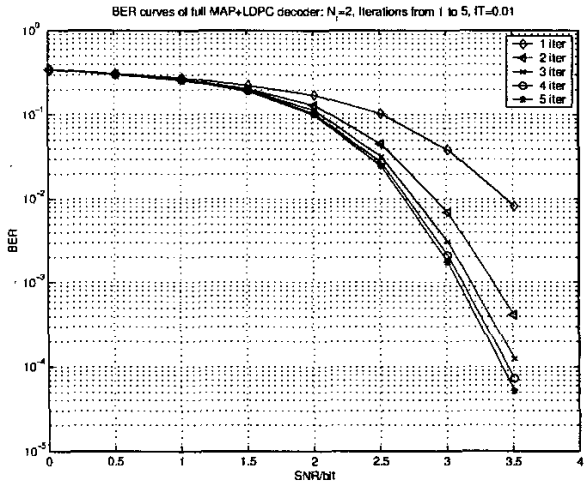


Fig. 5. BER of the full MAP-Bipartite on ($N_t = 2, L = 2$) channel, $f_{dm}T = 0.01$

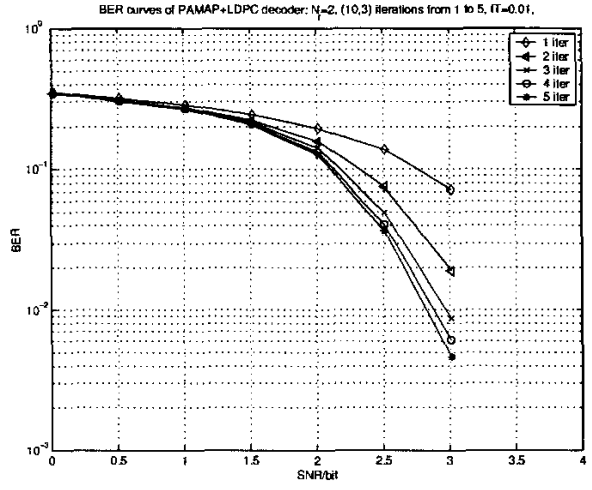


Fig. 6. BER of the PAMAP on ($N_t = 2, L = 2$) channel, $f_{dm}T = 0.01$

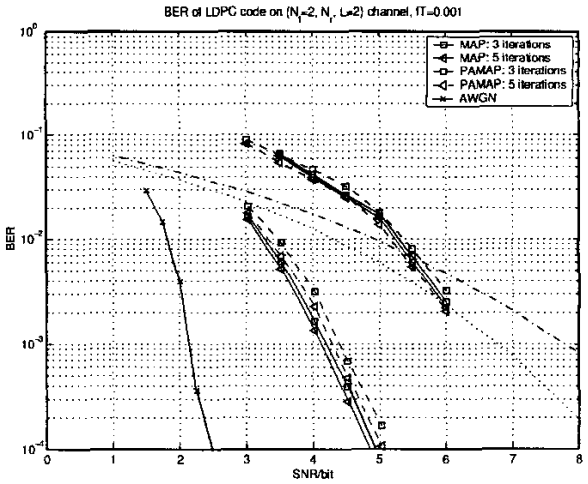


Fig. 7. BER on ($N_t = 2, N_r, L = 2$) channel, $f_{dm}T = 0.001$

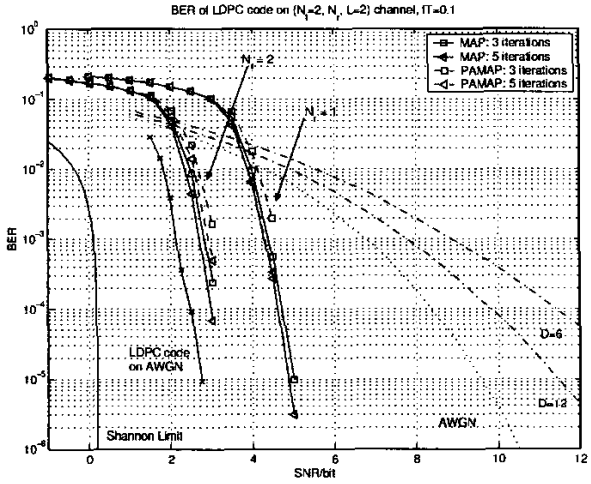


Fig. 8. BER on ($N_t = 2, N_r, L = 2$) channel, $f_{dm}T = 0.1$

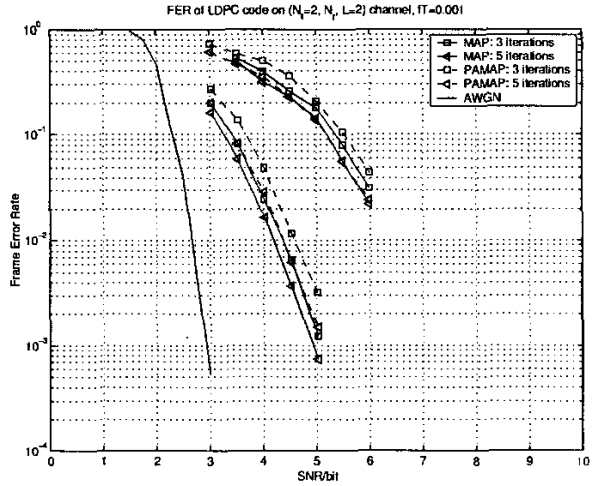


Fig. 9. FER on ($N_t = 2, N_r, L = 2$) channel, $f_{dm}T = 0.001$

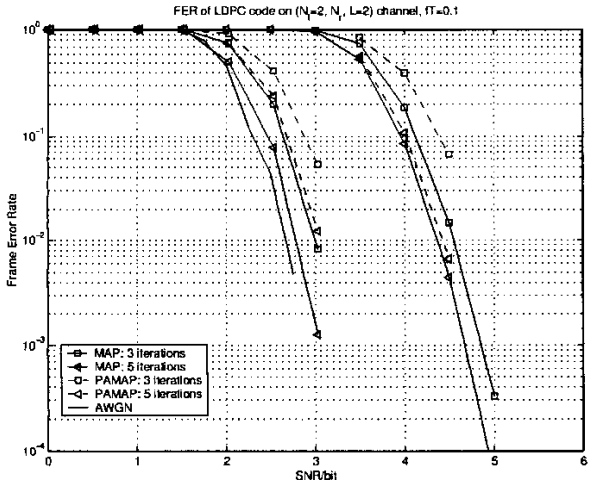


Fig. 10. FER on $(N_t = 2, N_r, L = 2)$ channel, $f_{dm}T = 0.1$

## REFERENCES


[1] J.G. Proakis, *Digital Communications*, McGraw-Hill, New York, 3rd edition, 1995.

[2] I.E. Telatar, "Capacity of multi-antenna gaussian channels," *AT&T Bell Labs. Tech. Memo*, 1995.

[3] G. Foschini and M. Gans, "On limits of wireless communications in a fading environment when using multiple antennas," *Wireless Personal Communications*, vol. 6, pp. 311–335, Mar. 1998.

[4] G. Foschini, G.D. Golden, R.A. Valenzuela, and P.W. Wolniansky, "Simplified processing for high spectral efficiency wireless communication employing multi-element arrays," *IEEE JSAC*, vol. 17, no. 11, pp. 1841–52, Nov. 1999.

[5] V. Tarokh, N.Seshadri, and A.R. Calderbank, "Space-time codes for high data rate wireless communications: Performance analysis and code construction," *IEEE Trans. Inform. Theory*, vol. 44, no. 5, pp. 744–65, March 1998.

[6] R.G. Gallager, *Low-density parity-check codes*, Ph.d. thesis, MIT, Cambrige, MA, 1963.

[7] Vivek Gulati and Heung no Lee, "A low-complexity iterative per-antenna map equalizer for mimo frequency-selecive fading channels," *Unpublished: Submitted to IEEE Globecom-2002*.

[8] D.J.C. Mackay, "Good error-correcting codes based on very sparse matrices," *IEEE Trans. Info. Theory*, vol. 45, no. 2, pp. 399–431, Mar. 1999.

[9] C. Berrou, A. Glavieux, and P. Thitimajshima, "Near Shannon limit error-correcting coding and decoding: Turbo-codes," in *Conference Record, IEEE International Conference on Communications, ICC-93*, May 1993, vol. 2, pp. 1064–1070.

[10] S. Benedetto and G. Montorsi, "Unveiling turbo codes: some results on parallel concatenated coding schemes," *IEEE Transactions on Information Theory*, vol. 42, no. 2, pp. 409–428, March 1996.

[11] M. Tuchler, R. Kotter, and A. Singer, "Turbo-equalization: Principles and new results," Submitted to IEEE Transactions on Communications, August 2000.

[12] N. D. Doan and R. M. A. P. Rajatheva, "Turbo equalization for non-binary coded modulation schemes over frequency selective fading channels," in *IEEE 51st Vehicular Technology Conference Proceedings, VTC-2000*, May 2000, vol. 3, pp. 2217–2221.

[13] K. R. Narayanan, U. Dasgupta, and B. Lu, "Low complexity turbo equalization with binary precoding," in *Conference Record, IEEE International Conference on Communications, ICC-2000*, June 2000, vol. 1, pp. 1–5.

[14] P. Magniez, P. Duhamel, A. Roumy, and I. Fijalkow, "Turbo-equalization applied to trellis-coded-modulations," in *Proceedings of IEEE 50th Vehicular Technology Conference, VTC-99*, September 1999, vol. 5, pp. 2556–2560.

[15] M. Tuchler, R. Koetter, and A. Singer, "Iterative correction of isi via equalization and decoding with priors," in *Proceedings of IEEE International Symposium on Information Theory, ISIT-2000*, June 2000, p. 100.

[16] P. Magniez, B. Muquet, P. Duhamel, and M. de Courville, "Improved Turbo-equalization, with applications to bit interleaved modulations," in *Conference Record of 34th Asilomar Conference on Signals, Systems and Computers*, November 2000, vol. 2, pp. 1786–1790.

[17] Y. Li and B. Chen, "Iterative decoding of serially concatenated convolutional codes over multipath intersymbol interference channels," in *Conference Record, IEEE International Conference on Communications, ICC-99*, June 1999, vol. 2, pp. 947–951.

[18] D. Raphaeli and Y. Zarai, "Combined turbo equalization and turbo decoding," *IEEE Communications Letters*, vol. 2, no. 4, pp. 107–109, April 1998.

[19] S. Benedetto, D. Divsalar, G. Montorsi, and F. Pollara, "Serial concatenation of interleaved codes: performance analysis, design, and iterative decoding," *IEEE Transactions on Information Theory*, vol. 44, no. 3, pp. 909–926, May 1998.

[20] J. Hagenauer, E. Offer, and L. Papke, "Iterative decoding of binary block and convolutional codes," *IEEE Trans. Info. Theory*, vol. 42, no. 2, pp. 429–45, March 1996.

[21] P. Robertson, E. Villebrun, and P. Hoeher, "A comparison of optimal and sub-optimal map decoding algorithms operating in the log domain," *Proc. of IEEE ICC-95*, vol. 2, pp. 1009–13, June 1995.

[22] S. Benedetto, D. Divsalar, G. Montorsi, and F. Pollara, "A soft-input soft-output APP module for iterative decoding of concatenated codes," *IEEE Communications Letters*, vol. 1, no. 1, pp. 22–24, January 1997.

[23] T.J. Richardson and R. Urbanke, "The capacity of low-density parity-check codes under message-passing decoding," *IEEE Trans. Infrom. Theory*, vol. 47, pp. 599–618, Feb 2001.

[24] H. El Gamal and Jr. A. R. Hammons, "Analyzing the turbo decoder using the Gaussian approximation," *IEEE Transactions on Information Theory*, vol. 47, no. 2, pp. 671–686, February 2001.

[25] D. Divsalar, S. Dolinar, and F. Pollara, "Iterative turbo decoder analysis based on density evolution," TMO Progress Report 42-144, JPL, NASA, February 15 2001.

[26] K. R. Narayanan, "Effect of precoding on the convergence of turbo equalization for partial response channels," *IEEE Journal on Selected Areas in Communications*, vol. 19, no. 4, pp. 686–698, April 2001.

[27] V. Tarokh, A. F. Naguib, and A. R. Calderbank, "Space-time codes for high data rate wireless communications: Performance criterion and code construction," *IEEE Transactions on Information Theory*, vol. 44, no. 2, pp. 744–765, March 1998.

[28] V. Tarokh, A. Naguib, N. Seshadri, and A. R. Calderbank, "Space-time codes for high data rate wireless communication: performance criteria in the presence of channel estimation errors, mobility, and multiple paths," *IEEE Transactions on Communications*, vol. 47, no. 2, pp. 199–207, February 1999.

[29] M. J. Heikkila, K. Majonen, and J. Lilleberg, "Decoding and performance of space-time trellis codes in fading channels with intersymbol interference," in *Proceedings of the 11th IEEE International Symposium on Personal, Indoor and Mobile Radio Communications*, 2000, vol. 1, pp. 490–494.

[30] G. Bauch and A. F. Naguib, "MAP equalization of space-time coded signals over frequency selective channels," in *Proceedings of Wireless Communications and Networking Conference, WCNC-99*, September 1999, vol. 1, pp. 261–265.

[31] Heung-No Lee and G.J. Pottie, "Fast adaptive equalization/diversity combining for time-varying dispersive channels," *IEEE Trans. on Commun.*, vol. 46, pp. 1146–62, Sept. 1998.

[32] L.R. Bahl, J. Cocke, F. Jelinek, and J. Raviv, "Optimal decoding of linear codes for minimizing symbol error rate," *IEEE Trans. Info. Theory*, vol. 20, pp. 284–7, Mar. 1974.